Colloids and Surfaces B: Biointerfaces 186 (2020) 110733

Contents lists available at ScienceDirect

Colloids and Surfaces B: Biointerfaces

journal homepage: www.elsevier.com/locate/colsurfb

Bioinspired DNA nanocockleburs for targeted delivery of doxorubicin

Si Sun[a,1], Nihad Cheraga[b,1], Han-Ning Jiang[b,1], Qian-Ru Xiao[b], Peng-Cheng Gao[a], Yang Wang[a], Ying-Ying Wei[a], Xiao-Wei Wang[c], Yong Jiang[a,*]

[a] School of Chemistry and Chemical Engineering, Jiangsu Province Hi-Tech Key Laboratory for Biomedical Research, Southeast University, Nanjing 211189, PR China
[b] State Key Laboratory of Bioelectronics, School of Biological Sciences and Medical Engineering, Southeast University, Nanjing 210096, PR China
[c] Department of Cardiovascular Surgery, The First Affiliated Hospital of Nanjing Medical University, Nanjing 210036, PR China

ARTICLE INFO

Keywords:
Self-assembly
DNA nanocockleburs
Target drug delivery
Aptamers

ABSTRACT

A variety of three-dimensional DNA assemblies have been proposed as drug carriers owing to their good biocompatibility and easy fabrication. In this study, inspired by the structure of cockleburs, a novel aptamer-tethered DNA assembly was developed for effective targeted drug delivery. The Apt-nanocockleburs were fabricated *via* a facile process of DNA base pairing: four complementary DNA single strands, including one aptamer-ended strand and three sticky-end strands, were applied to pair with each other. The main body of the nanocockleburs can load doxorubicin (Dox) whilst the covered aptamer spines bind to the target MCF-7 cells. The self-assembled Apt-nanocockleburs exhibit higher cell uptake as well as increased cytotoxicity to MCF-7 cells than DNA nanocockleburs without aptamers. This study provided a DNA constructing platform to produce new drug carriers with high selectivity for cancer targeted drug delivery.

1. Introduction

In the past decades, chemotherapy was the most common strategy to treat cancer, however, several challenges still remain due to poor drug efficacy, systematic toxicity and lack of specificity [1]. In order to overcome these issues, numerous studies have explored loading drugs into various nano-carriers having excellent biocompatibility and capable of specifically releasing the drug at the cancer site.

Recently, DNA nanostructure has emerged as a promising biomaterial for nano-carriers due to its good biocompatibility and the facile fabrication process. Previous studies showed that DNA can be used to construct three-dimensional polyhedra for cancer therapy [2–5]. In this context, our group has previously reported that gold nanoparticle corbelled DNA nanocage can be used as a nano-system for doxorubicin (Dox) controlled release [6]. Nevertheless, the preparation efficiency was relatively low and the whole delivery system was not cost-effective. Moreover, due to the limited cell penetration of oligonucleotides, the gold-DNA assemblies had a poor intracellular drug delivery [4].

Aptamer is a well-known single-stranded oligonucleotide evolved by a process called systematic evolution of ligands by exponential enrichment (SELEX) [7]. Its ability to bind to cancer cell's membrane would help nanoparticles or DNA assemblies to specially enter cancer cells [5,8–10]. Tan et al. [10] developed an aptamer tethered DNA nanotrain to deliver drug to target cells. To improve the amount of aptamers, Li et al. [11] designed a DNA nanocentipede which consisting several aptamers in one assembly. However, the high cost biotin modified DNA sequences hampered its application.

Cockleburs can be carried long distances from their parent plants by firmly sticking to the fur of animals because of their unique surface structure, which is covered with stiff and hooked spines. Inspired by the structure of cocklebur, we designed an aptamer-functionalized 3D DNA assembly (Apt-nanococklebur) for targeted delivery of Dox to Michigan Cancer Foundation-7 (MCF-7) breast cancer cells. Scheme 1 illustrated the fabrication method of Apt-nanocockleburs. In a one-pot hybridization process, four complementary single DNA strands (S1, S2, S3, and S4), of which one is an aptamer-ended and the other three are sticky-ended strands, assembled into sticky-ended four-point-star motif. Then the self-complementary sticky-ends of each four-point-star motif paired with other motifs' sticky-ends to further assemble into Apt-nanocockleburs. The multi-valent Apt-nanocockleburs are made from non-modified DNA which can decrease the cost as compared with DNA nanocentipedes [11].

As shown in Scheme 1, each single DNA strand has three different segments represented with different colors, and segments having the same color in different strands are complementary to each other. Despite the aptamer that contains 26 nucleotides, all other segments

* Corresponding author.
E-mail address: yj@seu.edu.cn (Y. Jiang).
[1] These authors contributed equally to this work.

https://doi.org/10.1016/j.colsurfb.2019.110733
Received 7 June 2019; Received in revised form 12 December 2019; Accepted 13 December 2019
Available online 14 December 2019

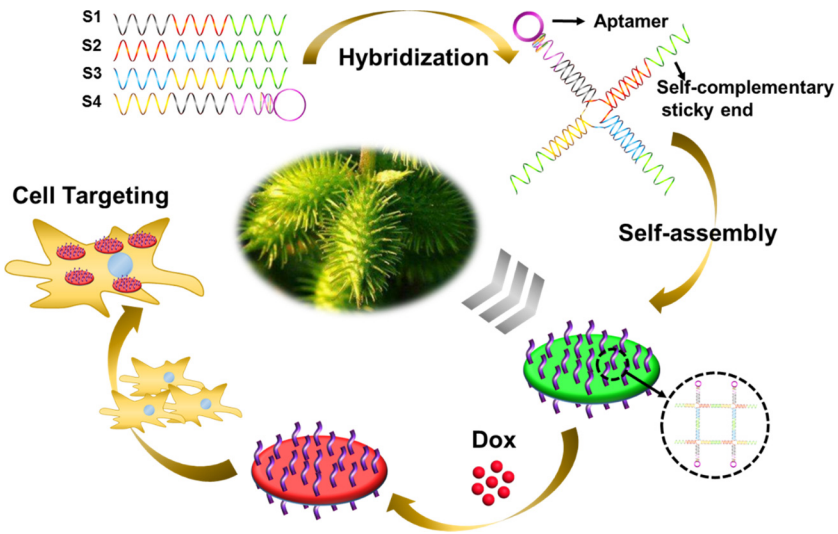

Scheme 1. Schematic illustration of the fabrication process of the Apt-nanocockleburs: In a one-pot hybridization process, four complementary single DNA strands (S1, S2, S3, and S4), of which one is an aptamer-ended and the other three are sticky-ended strands, assembled into sticky-ended four-point-star motif. Then the self-complementary sticky-ends of each four-point-star motif paired with other motifs' sticky-ends to further assemble into Apt-nanocockleburs.

contain 16 nucleotides each. The first segment of each strand is complementary to the middle one of the neighboring strand and points to the center of the four-point-star motif. Accordingly, the obtained four-point-star motif contains one aptamer end and three self-complementary sticky ends. In this study, AS1411 was used as an aptamer due to its well-known tumor target-ability through selective interaction with nucleolin (NCL) excessively expressed in cancer cells [12,13].

2. Experimental

2.1. Materials

Doxorubicin (Dox) was purchased from Solarbio Co. Ltd. (Beijing, China). PBS buffer, TAE buffer, Gel Red, high-glucose DMEM, yeast tRNA, trypsin-EDTA solution, and SYBR Green I were purchased from Sangon Biotech. Co. Ltd. (Shanghai, China). Agarose was purchased from Macklin Biochemical Co. Ltd. (Shanghai, China). Phosphotungstic acid and Dimethyl sulfoxide (DMSO) were purchased from Sinopharm Chemical Reagent Co., Ltd (Shanghai, China). Fetal bovine serum (FBS) was purchased from Wisent (Canada). Non-enzy cell detach solution was purchased from Applygen Co. Ltd. (Beijing, China). Bovine serum albumin (BSA) and $MgCl_2$ were purchased from Aladdin Industrial Co. (Shanghai, China). Lyso Tracker Blue was purchased from KeyGen Biotech. Co. Ltd. (Nanjing, China). (3-(4, 5-dimethylthiazolyl-2)-2, 5-diphenyltetrazolium bromide) MTT was purchased from Beyotime Biotech. Co. Ltd. (Shanghai, China). DNA sequences were purchased from Sangon Biotech. Co. Ltd. (Shanghai, China) and listed in Table 1. MCF-7 cells and HFF cells were obtained from the Chinese Academy of Sciences Cells Bank. All chemicals were used as received. Ultrapure water used in this experiment was distilled.

Table 1
Sequences of DNA Probes.

Probes	Sequences (5'-3')
S1	ATAGTGAGTCGTATTAATTAACCCTCACTAAAA AGGATCCGGATCCTT
S2	TTTAGTGAGGGTTAATCATACGATTTAGGTGAA AGGATCCGGATCCTT
S3	TCACCTAAATCGTATGGGAGCTCTGCTTATATA AGGATCCGGATCCTT
S4	GGTGGTGGTGGTTGTGGTGGTGGTGGTTTTTT TATCACTCAGCATAATCCTCGAGACGAATATA
S5	TATCACTCAGCATAATCCTCGAGACGAATATA
FITC-S2	FITC-TTTAGTGAGGGTTAATCATACGATTTAG GTGAAAGGATCCGGATCCTT

2.2. Preparation of Apt-nanocockleburs

To prepare Apt-nanococklebur, DNA sequences S1, S2, S3 and S4 (or S5) were dissolved in PBS solution to reach a final concentration of 50 μM, respectively. Subsequently, 10 μL of each sample was diluted tenfold in PBS solution. The mixture was heated to 95 °C for 3 min with a PCR-cycler (Eppendorf AG 22331 Hamburg) and then cooled to room temperature (25 °C) with a rate of 1 °C per minute. Another 24 h was taken to complete the annealing process. Similarly, FITC-labeled Apt-nancockleburs were prepared, except that S2 was labeled with FITC.

2.3. Preparation of Dox-loaded Apt-nanocockleburs

To prepare Dox-loaded Apt-nanocockleburs, 2 μM Dox was incubated with different concentrations of Apt-nanocockleburs (0, 25, 50, 100, 250 and 500 nM) at room temperature for 2 h. The Dox intercalated samples were analyzed by using fluorescence spectrometry (excitation wavelength: 490 nm) with a Horiba Fluoromax-4 fluorescence spectrometer.

2.4. Agarose gel electrophoresis analysis

3 % agarose gel electrophoresis was proceeded at room temperature under 90 V. The gel was prepared in 30 mL 1 × TAE buffer and stained with 3 μL Gel Red. Results of the electrophoresis were analyzed by Kodak Gel Logic 112 imaging system.

2.5. Morphology characterization

For atomic force microscopy (AFM) characterization, the prepared Apt-nanocockleburs were first diluted 100 fold in 10 mM $MgCl_2$ solution. Then 20 μL sample were dripped onto a new cleaved mica. After 5 min, the mica was washed 5 times with 500 μL pure water and dried by nitrogen gas. Finally, the sample was analyzed with the Atomic Force Microscope (Bruker Inc.). The dynamic light scattering (DLS) characterization was performed on Brookhaven NanoBrook Omni instrument.

2.6. Cell culture

High-glucose DMEM with 10 % fetal bovine serum (FBS) was used for both MCF-7 cells and HFF cells. All cells were cultured in an atmosphere of 95 % air and 5 % CO_2 at 37 °C in a standard cell incubator.

2.7. Flow cytometry analysis

MCF-7 cells or HFF cells were seeded in cell culture dishes for 24 h. Then they were digested with non-enzy cell detach solution and suspended in binding buffer (PBS solution containing 0.1 mg/mL yeast tRNA, 1 mg/mL BSA, 4.5 g/L glucose and 5 mM $MgCl_2$) or cell culture medium. Next, cells were incubated with DNA samples at 4 °C for 30 min and washed with washing buffer (PBS solution containing 4.5 g/L glucose and 5 mM $MgCl_2$). Finally, the treated cells were analyzed with a BD Biosciences Accuri C6 flow cytometry.

2.8. Laser confocal scanning microscopic analysis

The fluorescence experiment was carried out with an Olympus FV3000 Laser confocal scanning microscope with a 60× oil immersion lens. First, DNA samples were dyed with SYBR Green I for 10 min and washed by centrifugation in Millipore filters. Cells cultured in 35 mm confocal dish were incubated with SYBR Green I-dyed DNA samples at 37 °C for 2 h. Then, the cells were washed twice with washing buffer and dyed with Lyso Tracker Blue for 10 min. Finally, the treated cells were washed twice and suspended in 1 mL binding buffer for observation.

2.9. Cell viability assay

In vitro cytotoxicity was determined using the colorimetric MTT assay analysis. First, MCF-7 cells and HFF cells were incubated with Dox-loaded DNA samples or free dox in culture medium for 48 h. Then the whole medium was removed and 100 μL fresh culture medium containing 10 μL (5 mg/mL in PBS) MTT solution was added into each well and incubated for another 4 h in the incubator (37 °C, 5 % CO_2). Next, the supernatant was discarded and 150 μL DMSO was added into each well to dissolve the formazan crystals. Finally, the analysis was performed using a Thermo Go Microplate Absorbance Reader at 490 nm. Cell viability (%) was calculated according to the following equation:

$$(At\text{-}Ac)/(Au\text{-}Ac) \times 100\ \%$$

where At, Au, Ac represent the absorbance of the treated wells, untreated wells and control wells, respectively. All tests were done in quadruplicate and the results were given as mean ± SEM.

3. Results and discussion

3.1. Agarose gel electrophoresis and morphology analysis

The assembled Apt-nanocockleburs were characterized by agarose gel electrophoresis and AFM. The results of the agarose gel electrophoresis are shown in Fig. 1(A). Lane 1 contains low molecular weight DNA markers (from 25 bp to 500 bp). Lane 2 to lane 4 contain band I, band II, and band III produced by single DNA strands S1, S2 and S3, respectively. Since these three sequences had similar molecular weight, their corresponding bands appeared at similar positions on each lane. However, band IV in lane 5 produced by S4 exhibited higher electrophoretic mobility than the first three strands. This could be explained by the addition of aptamer end, G-rich AS1411 segment [14], which improved the electrophoretic mobility of S4 DNA strand. The Apt-nanocockleburs exhibited a broad tailing band in line 6 due to the different molecular weight of the four assembled DNA sequences.

AFM was used to visualize the morphology of the assembled DNA nanocockleburs, and the images are displayed in Fig. 1(B) and (D). The results showed that DNA nanocockleburs of different sizes were formed. The size range calculated from Fig. 1(B) was from 20 nm to 40 nm. Moreover, Fig. 1(D) shows that the height of the DNA nanocockleburs was about 1.5 nm. Therefore, it was deduced that these nanocockleburs have sheet-like shape. Compared to sphere-like structure, sheet-like structure is more beneficial for drug loading because DNA strands would be exposed outside rather than encapsulated. Meanwhile, the DLS result (Fig. 1(C)) reveals that the assembled DNA nanocockleburs possesses an apparent hydrodynamic diameter of 62.5 ± 10 nm. The different state of the nanocockleburs accounts for the different diameters. AFM was performed under a dry state, while the DLS was performed under hydration [15,16], which lead to a larger size. The above results demonstrate that the Apt-nanocockleburs were successfully synthesized as designed.

3.2. Selective recognition ability of Apt-nanocockleburs in binding buffer

The selective binding ability of the Apt-nanocockleburs to target NCL-positive MCF7 cells was determined by flow cytometric analysis. Human Foreskin Fibroblast (HFF) were used as NCL-negative cells [17–19]. S2 DNA strand labeled with FITC was used as the fluorescent sequence in the Apt-nanocockleburs. MCF-7 cells and HFF cells were both incubated with a mixed solution of S1, FITC-S2 and S3 (Sample A), Non-apt-nanocockleburs (Sample B) or Apt-nanocockleburs solution (Sample C) in binding buffer at 4 °C for 30 min. Then, the samples were analyzed by flow cytometry after washing. The results are shown in Fig. 2(A, B). Only MCF-7 cells that have been incubated with the Apt-nanocockleburs showed significant fluorescence increase, suggesting a strong cell binding ability of the Apt-nanocockleburs [5,20]. On the other hand, the binding selectivity of these DNA assemblies was demonstrated on NCL-negative HFF cells. As shown in Fig. 2(B), no fluorescence changes were observed proving the lack of cell binding. This further demonstrates the selective binding ability of the Apt-nanocockleburs to MCF-7 cells.

3.3. Selective recognition ability of Apt-nanocockleburs in imitated physiological environment

To further study the selectivity of Apt-nanocockleburs in a more physiological environment, cell culture medium with 10 % FBS was used to simulate a physiological environment [11]. Briefly, MCF-7 cells and HFF cells were incubated with the mixed solution of S1, FITC-S2 and S3 (Sample A), Non-apt-nanocockleburs (Sample B) or Apt-nanocockleburs (Sample C) in the cell culture medium at 37 °C for 30 min. Results in Fig. 3(A) and (B) showed that MCF-7 cells treated with the Apt-nanocockleburs had a significant fluorescence enhancement, while no fluorescence changes were observed for HFF cells treated with different samples. These results are in accordance with those described in the previous section (Fig. 2), suggesting that the Apt-nanocockleburs could maintain its selective binding ability in a physiological environment.

All the above results demonstrated that the Apt-nanocockleburs have a strong binding affinity to MCF-7 cells whether in binding buffer or cell culture medium.

3.4. Time-dependent cellular internalization of the Apt-nanocockleburs

Cellular internalization is a crucial step for effective intercellular delivery of chemotherapeutic drugs. Herein, we investigated the Apt-nanocockleburs cellular internalization into MCF-7 cells by laser confocal scanning microscopy (LCSM). Considering that the fluorescence of Dox would quench after loading into DNA double strands, SYBR Green I, which can specifically bind to double-stranded DNA [21], was used as a fluorescent dye in order to track the internalization of Apt-nanocockleburs. More, Lyso Tracker Blue was used to stain lysosomes. The results in Fig. 4 revealed that SYBR Green I fluorescence gradually increased when the incubation time increased. These results are consistent with previous work [9,11], indicating that the Apt-nanocockleburs were uptaken by MCF-7 cells gradually. Moreover, the green fluorescence co-localized with the blue fluorescence, suggesting that

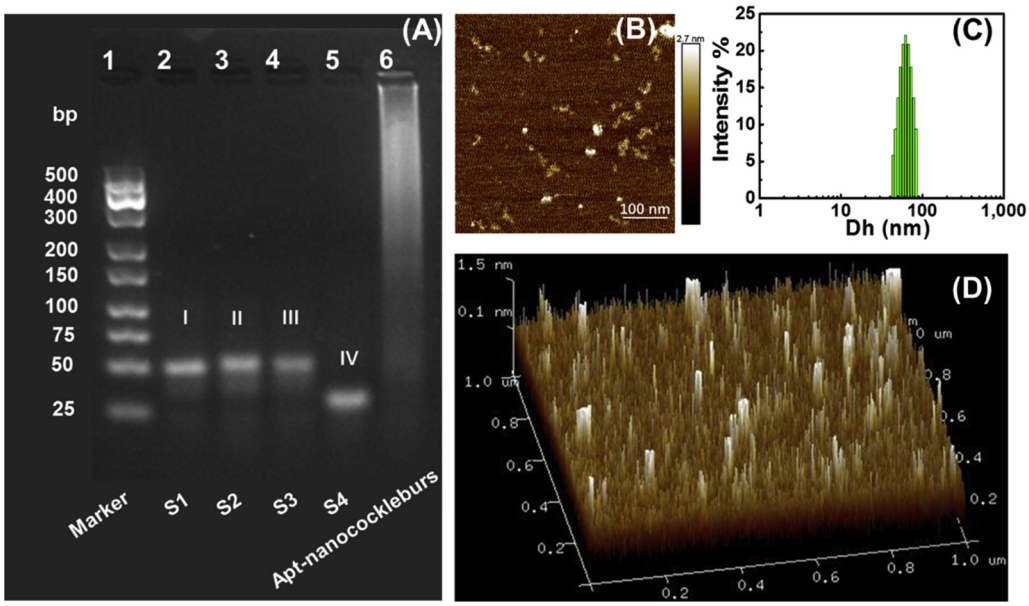

Fig. 1. Characterization of Apt-nanocockleburs. (A) Results of the agarose gel electrophoresis analysis. Lane 1: low molecular weight DNA marker (from 25 bp to 500 bp). Lane 2 to lane 5: single DNA strand (S1, S2, S3 and S4). Lane 6: DNA nanocockleburs. (B) AFM images of the Apt-nanocockleburs. (C) Hydrodynamic size of the Apt-nanocockleburs. (D) Heights of the Apt-nanocockleburs. Scale bar: 100 nm.

the Apt-nanocockleburs were localized in cytoplasm [22].

3.5. Selective cellular internalization of the Apt-nanocockleburs

To further investigate the selective cellular internalization of the Apt-nanocockleburs, MCF-7 cells were incubated with SYBR Green I dyed Apt-nanocockleburs or SYBR Green I dyed non-Apt-nanocockleburs for 2 h. On the other hand, HFF cells were also incubated with the SYBR Green I dyed Apt-nanocockleburs. As shown in Fig. 5, the green fluorescence of MCF-7 cells treated with the Apt-nanocockleburs was much stronger compared to the one of MCF-7 cells treated with non-Apt-nanocockleburs. Whereas HFF cells treated with the SYBR Green I dyed Apt-nanocockleburs exhibited little green fluorescence. These results were consistent with the results of flow cytometry, proving that the Apt-nanocockleburs had selectivity to MCF-7 cells. Moreover, as illustrated before, the fluorescence of the Lyso Tracker Blue and the SYBR Green I overlapped, suggesting that the Apt-nanocockleburs were internalized by MCF-7 cells. Taken together, it was demonstrated that the Apt-nanocockleburs could be specifically internalized by the targeted cancer cells.

3.6. Dox loading capacity of the Apt-nanocockleburs

The drug-loading ability of Apt-nanocockleburs were also studied. Theoretically, each paired S1, S2, S3 and S4 can provide 28 sites for Dox molecules. When dox is loaded into double DNA strands, its fluorescence would quench [10], thereby, fluorescence spectrophotometer was used to determine dox-loading capacity of Apt-nanocockleburs. Briefly, 2 μM Dox were incubated with series of concentrations of Apt-nanocockleburs ranging from 25 nM to 500 nM. As shown in Fig. 6, when the concentration of Apt-nanocockleburs increased, the fluorescence intensity of Dox decreased accordingly. However, the fluorescence intensity dropped intensely when the concentration of the Apt-nanocockleburs reached 100 nM. Interestingly, the spectra of both 250 nM and 500 nM were similar to the one of 100 nM, suggesting that Apt-nanocockleburs at a concentration of 100 nM is enough to load 2 μM of Dox. Theoretically, 100 nM Apt-nanocockleburs can load 2.3 μM Dox. The above results reveal that the drug-loading efficiency of Apt-nanocockleburs is 87 %.

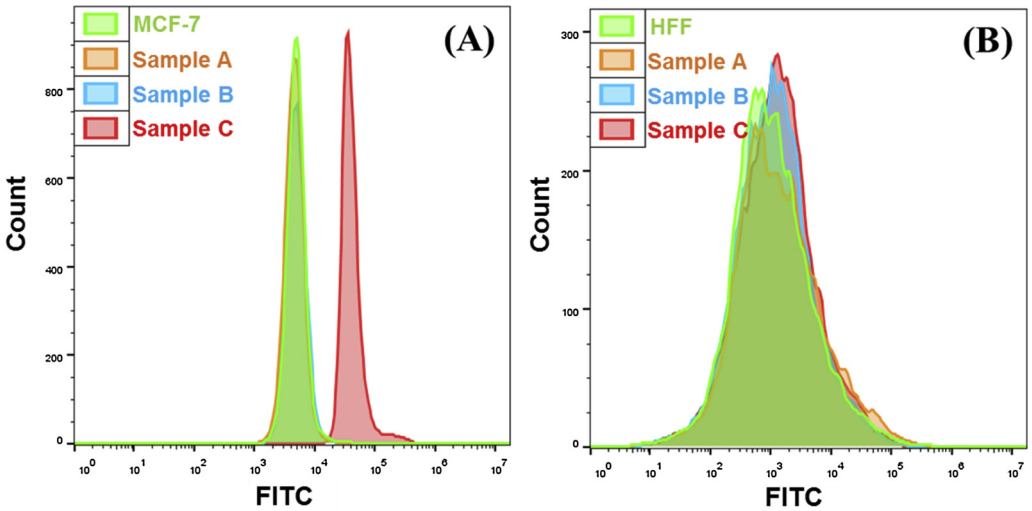

Fig. 2. Flow cytometry characterization of the binding affinity and selectivity of Apt- nanocockleburs to the target MCF-7 cells (A) and non-target HFF cells (B) in the binding buffer. Sample A: mix solution of S1, S2 and S3; Sample B: Non-apt-nanocockleburs; Sample C: Apt-nanocockleburs.

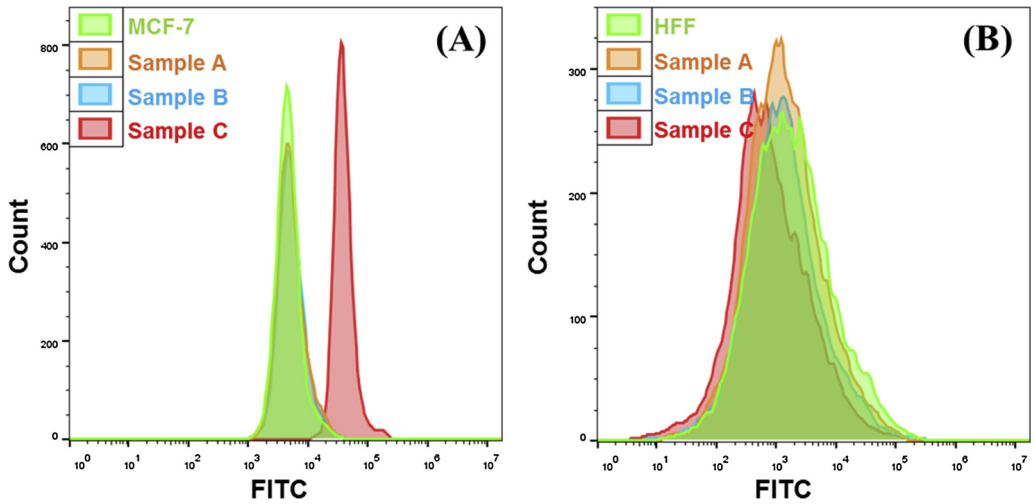

Fig. 3. Flow cytometry characterization of the binding affinity and selectivity of Apt-nanocockleburs to the target MCF-7 cells (A) and non-target HFF cells (B) in culture medium. Sample A: mix solution of S1, S2 and S3; Sample B: Non-apt-nanocockleburs; Sample C: Apt-nanocockleburs.

3.7. Cellular cytotoxicity of drug delivery by Apt-nanocockleburs

Finally, the cellular cytotoxicity of the Apt-nanocockleburs-Dox against Non-apt-nanococklebur-Dox and free Dox was examined on target MCF-7 cells and HFF cells by MTT assay. Cellular cytotoxicity assay was conducted at dox dose of 5 μM. This dose was chosen as the effective therapeutic dose based on previous studies [4,11,23]. In addition, the cytotoxicity of the Apt-nanocockleburs (1 μM) without Dox was also studied.

The results in Fig. 7(A) revealed that the cytotoxicity of Apt-nanococklebur-Dox in MCF-7 cells is significantly higher than that of Non-apt-nanococklebur-Dox, suggesting greater intracellular targeted delivery. On the other hand, both the Apt-nanococklebur-Dox and the Non-apt-nanococklebur-Dox showed relatively low cytotoxicity in HFF cells. This could be attributed to the limited cellular internalization due to the low cell binding of Apt-nanococklebur-Dox for HFF cells. However, the free dox showed high cytotoxicity to both MCF-7 cells and HFF cells. In addition, the cytotoxic results of different concentrations of Dox-loaded Apt-nanocockleburs in Fig. 7(B) further proved the high selectivity of Apt-nanocockleburs. In addition, the Apt-nanocockleburs showed low cytotoxicity on both cells even at a high dose of 1 μM, demonstrating its good biocompatibility. These results indicated that Apt-nanocockleburs-Dox had a selective cytotoxicity to the targeted cells and a reduced cytotoxicity to non-target cells. Therefore, Apt-nanocockleburs might be used as safe carrier for cancer targeting drug delivery.

4. Conclusions

In conclusion, a novel cocklebur inspired nanocarrier for Dox targeted delivery has been developed. The Apt-nanocockleburs showed improved cellular internalization and selective binding when compared to DNA nanocockleburs without aptamer covering. Flow cytometry demonstrated that the Apt-nanocockleburs might have significant binding affinity to MCF-7 cells whether in binding buffer or cell culture medium. In addition, the Apt-nanococklebur-Dox showed increased cytotoxicity when compared with Non-apt-nanococklebur-Dox in MCF-7 cells target cells. This constructed DNA nanoplatform could be used as

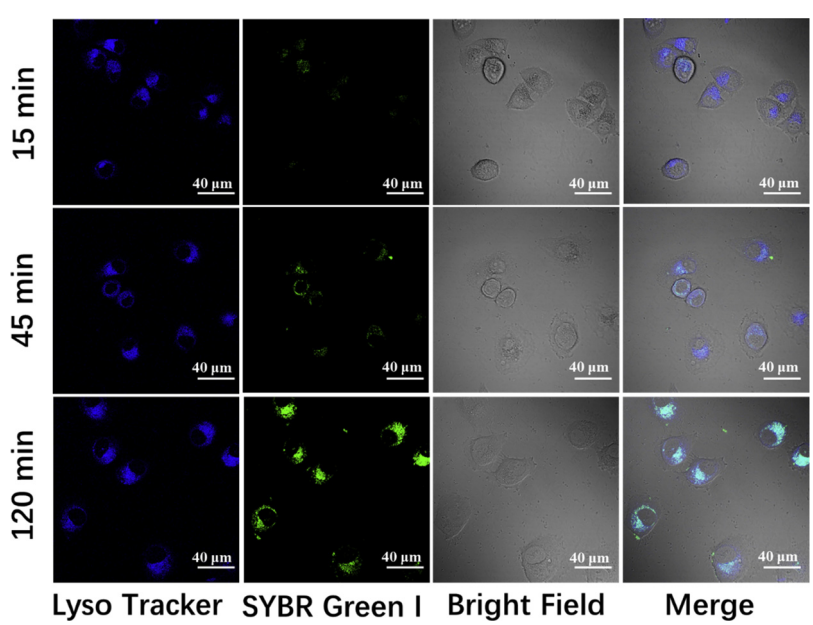

Fig. 4. Laser confocal scanning microscopy characterization of the time-dependent cellular internalization of the Apt-nanocockleburs. MCF-7 cells were incubated at 37 °C for 15 min, 45 min, and 120 min respectively. Scale bars: 40 μm.

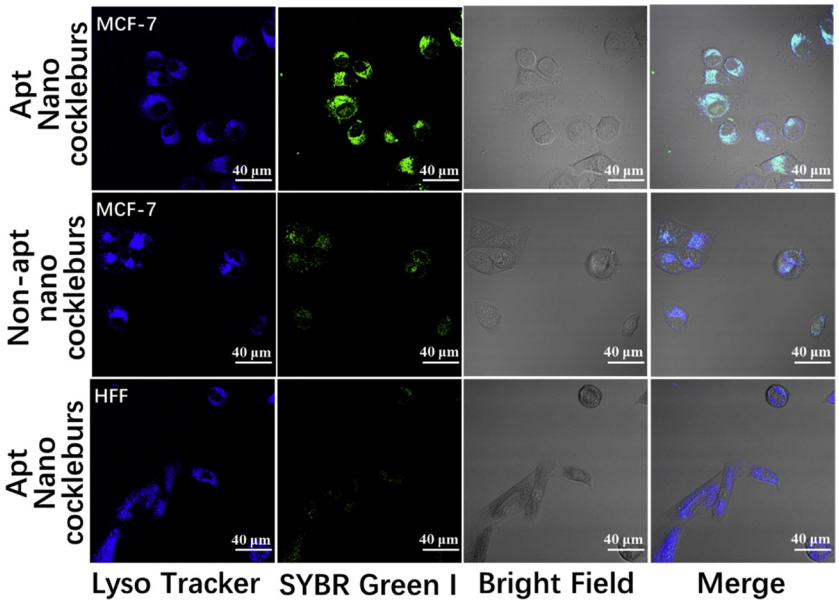

Fig. 5. Laser confocal scanning microscopy characterization of the cellular internalization of the Apt-nanocockleburs in different cells and Non-Apt-nanocockleburs in MCF-7 cells. MCF-7 cells and HFF cells were incubated at 37 °C 120 min. Scale bars: 40 μm.

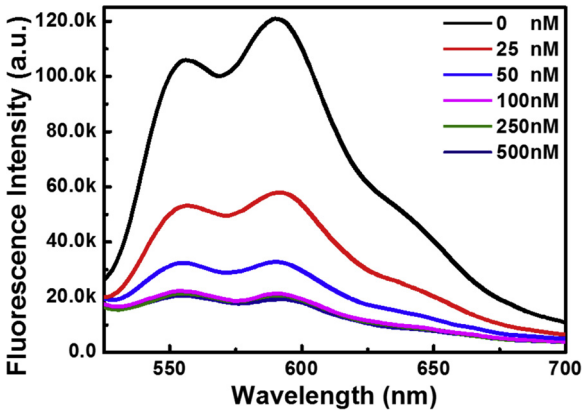

Fig. 6. Characterization of Dox-loading capacity of Apt-nanocockleburs by fluorescence spectra.

a new carrier for cancer targeted drug delivery.

Author contributions section

Si Sun contributed to the main experiments and writing. Nihad Cheraga and Qian-Ru Xiao helped to revise the language and writing. Han-Ning Jiang helped to analyze AFM. Peng-Cheng Gao, Yang Wang and Ying-Ying Wei helped to prepared the materials and some experiments. Xiao-Wei Wang and Yong Jiang helped to guide the project.

Declaration of Competing Interest

The authors declare that they have no known competing financial interests or personal relationships that could have appeared to influence the work reported in this paper.

Acknowledgements

This work was supported by the Project Funded by the Priority Academic Program Development of Jiangsu Higher Education Institutions (PAPD), the Fundamental Research Funds for the Central

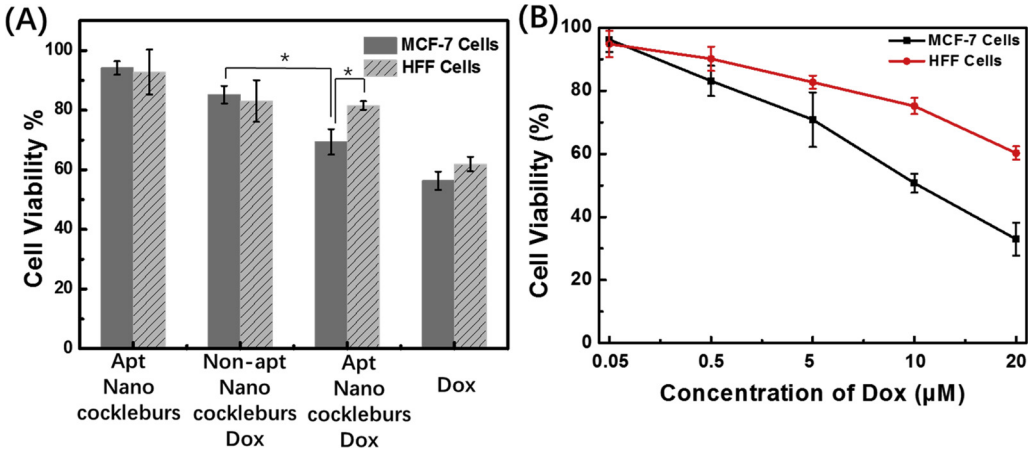

Fig. 7. Cytotoxicity of (A) different products and (B) Dox-loaded Apt-nanocockleburs to MCF-7 cells and HFF cells by MTT assay. (mean ± SEM). Data is analyzed using the ANOVA model, *$p < 0.05$.

Universities with grant number 2242016K41020 and the National Natural Science Foundation of China (NSFC) with grant number 81573234.

References

[1] M.M. Gottesman, T. Fojo, S.E. Bates, Multidrug resistance in cancer: role of ATP–dependent transporters, Nat. Rev. Cancer 2 (2002) 48–58.
[2] Y. He, T. Ye, M. Su, C. Zhang, A.E. Ribbe, W. Jiang, C. Mao, Hierarchical self-assembly of DNA into symmetric supramolecular polyhedra, Nature 452 (2008) 198–201.
[3] Y. Zhang, N.C. Seeman, Construction of a DNA-truncated octahedron, J. Am. Chem. Soc. 116 (1994) 1661–1669.
[4] M. Chang, C.-S. Yang, D.-M. Huang, Aptamer-conjugated DNA icosahedral nanoparticles as a carrier of doxorubicin for cancer therapy, ACS Nano 5 (2011) 6156–6163.
[5] J. Li, H. Pei, B. Zhu, L. Liang, M. Wei, Y. He, N. Chen, D. Li, Q. Huang, C. Fan, Self-assembled multivalent DNA nanostructures for noninvasive intracellular delivery of immunostimulatory CpG oligonucleotides, ACS Nano 5 (2011) 8783–8789.
[6] Z.-M. Zhang, P.-C. Gao, Z.-F. Wang, B.-W. Sun, Y. Jiang, DNA-caged gold nanoparticles for controlled release of doxorubicin triggered by a DNA enzyme and pH, Chem. Commun. 51 (2015) 12996–12999.
[7] K. Sefah, D. Shangguan, X. Xiong, M.B. O'donoghue, W. Tan, Development of DNA aptamers using cell-SELEX, Nat. Protoc. 5 (2010) 1169–1185.
[8] D. Kim, Y.Y. Jeong, S. Jon, A drug-loaded aptamer-gold nanoparticle bioconjugate for combined CT imaging and therapy of prostate cancer, ACS Nano 4 (2010) 3689–3696.
[9] S. Yu, R. Dong, J. Chen, F. Chen, W. Jiang, Y. Zhou, X. Zhu, D. Yan, Synthesis and self-assembly of amphiphilic aptamer-functionalized hyperbranched multiarm copolymers for targeted cancer imaging, Biomacromolecules 15 (2014) 1828–1836.
[10] G. Zhu, J. Zheng, E. Song, M. Donovan, K. Zhang, C. Liu, W. Tan, Self-assembled, aptamer-tethered DNA nanotrains for targeted transport of molecular drugs in cancer theranostics, Proc. Natl. Acad. Sci. 110 (2013) 7998–8003.
[11] W. Li, X. Yang, L. He, K. Wang, Q. Wang, J. Huang, J. Liu, B. Wu, C. Xu, Self-assembled DNA nanocentipede as multivalent drug carrier for targeted delivery, ACS Appl. Mater. Interfaces 8 (2016) 25733–25740.
[12] P.J. Bates, E.M. Reyes-Reyes, M.T. Malik, E.M. Murphy, M.G. O'toole, J.O. Trent, G-quadruplex oligonucleotide AS1411 as a cancer-targeting agent: uses and mechanisms, Biochim. Biophys. Acta (BBA)-Gen. Subj. (2016).
[13] J. Li, C.-Y. Hong, S.-X. Wu, H. Liang, L.-P. Wang, G. Huang, X. Chen, H.-H. Yang, D. Shangguan, W. Tan, Facile phase transfer and surface biofunctionalization of hydrophobic nanoparticles using janus DNA tetrahedron nanostructures, J. Am. Chem. Soc. 137 (2015) 11210–11213.
[14] R. Frank, H. Koster, DNA chain-length markers and the influence of base composition on electrophoretic mobility of oligodeoxyribonucleotides in polyacrylamide-gels, Nucleic Acids Res. 6 (1979) 2069–2087.
[15] Q. Lu, Y.-F. Meng, P.-C. Gao, J. Wei, S. Sun, J.-J. Zhou, Z.-F. Wang, Y. Jiang, A pH responsive micelle combined with Au nanoparticles for multi-stimuli release of both hydrophobic and hydrophilic drug, RSC Adv. 6 (2016) 58654–58657.
[16] X. Ji, Y. Li, H. Wang, R. Zhao, G. Tang, F. Huang, Facile construction of fluorescent polymeric aggregates with various morphologies by self-assembly of supramolecular amphiphilic graft copolymers, Polym. Chem. 6 (2015) 5021–5025.
[17] H. Motaghi, M.A. Mehrgardi, P. Bouvet, Carbon dots-AS1411 aptamer nanoconjugate for ultrasensitive spectrofluorometric detection of cancer cells, Sci. Rep. 7 (2017) 10513.
[18] E. Kocisova, P. Praus, J. Bok, S. Bonneau, F. Sureau, Intracellular monitoring of AS1411 aptamer by time-resolved microspectrofluorimetry and fluorescence imaging, J. Fluoresc. 25 (2015) 1245–1250.
[19] M. Keshtkar, D. Shahbazigahrouei, S.M. Khoshfetrat, M.A. Mehrgardi, M. Aghaei, Aptamer-conjugated magnetic nanoparticles as targeted magnetic resonance imaging contrast agent for breast cancer, J. Med. Signals Sens. 6 (2016) 243–247.
[20] L. Qiu, T. Chen, I. Oçsoy, E. Yasun, C. Wu, G. Zhu, M. You, D. Han, J. Jiang, R. Yu, A cell-targeted, size-photocontrollable, nuclear-uptake nanodrug delivery system for drug-resistant cancer therapy, Nano Lett. 15 (2014) 457–463.
[21] H. Zipper, H. Brunner, J. Bernhagen, F. Vitzthum, Investigations on DNA intercalation and surface binding by SYBR Green I, its structure determination and methodological implications, Nucleic Acids Res. 32 (2004) e103.
[22] L. He, X. Yang, F. Zhao, K. Wang, Q. Wang, J. Liu, J. Huang, W. Li, M. Yang, Self-assembled supramolecular nanoprobes for ratiometric fluorescence measurement of intracellular pH values, Anal. Chem. 87 (2015) 2459–2465.
[23] V. Bagalkot, O.C. Farokhzad, R. Langer, S. Jon, An aptamer-doxorubicin physical conjugate as a novel targeted drug-delivery platform, Angew. Chemie Int. Ed. 45 (2010) 8149–8152.